Int J Clin Exp Pathol 2018;11(11):5278-5289
www.ijcep.com /ISSN:1936-2625/IJCEP0085511

Original Article

Aconitine inhibits the proliferation of hepatocellular carcinoma by inducing apoptosis

Xiuzhong Qi[1], Lin Wang[2], Huan Wang[2], Ling Yang[3], Xia Li[2], Lina Wang[2]

[1]Department of Traditional Chinese Medicine, The Qingdao First Sanitarium of Navy, Qingdao, PR China; [2]Department of Traditional Chinese Medicine, Changhai Hospital, Naval Medical University, Shanghai, PR China; [3]Vocational Education College, Dezhou University, Dezhou, PR China

Received September 14, 2018; Accepted September 25, 2018; Epub November 1, 2018; Published November 15, 2018

Abstract: Hepatocellular carcinoma (HCC) is the primary liver cancer that occurs with a high incidence in Asia. Owing to the poor prognosis of the disease, the mortality rate remains high, making HCC the third most common cause of cancer-related mortality worldwide. Studies on current therapies have generated little empirical evidence in improving the survival rate of patients with advanced HCC. Certain agents have exhibited promising results in molecular targeted therapy, but they remain in clinical trials. Aconitine, a main bioactive constituent of a traditional Chinese herb, Wutou, and belonging to the *Aconitum* genus, has been demonstrated to inhibit the growth of certain tumors, including HCC, but the underlying molecular mechanism by which aconitine inhibits tumor growth is largely unknown. In the present study, aconitine was applied to two types of hepatic carcinoma cells and normal hepatic cells at various concentrations, and it was found to specifically inhibit the proliferation of cancer cells in a dose-dependent manner. Further study found that aconitine activated the production of reactive oxygen species, leading to an increased release of cytochrome *c* from mitochondria and the activation of apoptosis. This is demonstrated by the increased cleavage of caspases 3 and 7, as well as an increased B-cell lymphoma 2 (Bcl-2)-associated X protein level and a decreased Bcl-2 level in cancer cells. An *in vivo* study also found that aconitine was able to inhibit the growth of tumors in mice. The results of the present study suggest that aconitine has the potential to be developed into an effective anti-HCC agent.

Keywords: Aconitine, aconitum, diterpenoid alkaloids, hepatocellular carcinoma, apoptosis, reactive oxygen species

Introduction

Hepatocellular carcinoma (HCC) accounts for the majority of liver cancers and is therefore also called primary liver cancer. It is the fifth most common cancer in males and the seventh in females globally. This type of cancer occurs at a particularly high rate in Asia, and the rates have increased between 2- and 3-fold in males compared with in females [1]. Owing to the poor prognosis of the disease, the mortality rate is almost the same as the number of novel cases (~598,000) annually, making HCC the third most common cause of cancer-associated mortality worldwide [2]. Currently, the treatment for HCC includes systemic therapy, hormonal therapy, chemotherapy and molecularly targeted therapy [3-5]. However, despite decades of investigation, there is no empirical evidence demonstrating that systemic chemotherapy or hormonal therapy has improved the survival rate of patients with advanced HCC. Molecularly targeted therapy has exhibited certain exciting developments with a number of promising agents, including sunitinib and brivanib, which remain in Phase III clinical trials [6].

Recently, owing to the effect of inhibiting tumor growth and decreasing the rate of tumor recurrence and metastasis, Chinese medicine has gained attention in the investigation of cancer therapy. The root of *Aconitum carmichaelii* Debx (Ranunculaceae) is a traditional Chinese herb also known as Wutou present mainly in Jiangyou of the Sichuan province in China. Wutou has long been used as an analgesic and anti-inflammatory agent [1]. In combination

with other Chinese herbs, Wutou has also been used in the treatment of cancer in Chinese medicine [7-10]. Furthermore, it has been reported that extracts of Wutou alone are able to inhibit the proliferation of lung cancer *in vitro* [11, 12]. The main bioactive constituents of plants from the *Aconitum* genus are diterpenoid alkaloids that belong to the C_{18}, C_{19} and C_{20} subtypes of alkaloids [2] and have attracted interest owing to their antitumor activity [3, 4]. Of these diterpenoid alkaloids, aconitine has been identified as a constituent of anticancer agents [13, 14]. Recently, aconitine has been demonstrated to inhibit the proliferation and invasiveness of breast cancer cells by blocking the phosphoinositide 3-kinase (PI3K)/protein kinase B (Akt) signaling pathway [15]. In melanoma cells, aconitine inhibits the PI3K/Akt and mitogen-activated protein kinase/extracellular-signal-regulated kinase 1/2 signaling pathways, induces apoptosis and therefore inhibits the proliferation of melanoma cells [16]. Injection of aconitine-based anticancer drugs significantly decreased the symptoms of HCC with minimal side effects [17]. Despite the progress being made in applying aconitine in the treatment of HCC, the molecular mechanism by which aconitine inhibits the growth of HCC remains largely unknown.

Reactive oxygen species (ROS) are chemically reactive molecules containing oxygen. They are formed as natural byproducts of the normal metabolism of oxygen and serve important roles in cell signaling [18]. ROS are normally generated from mitochondria and are destructive to both DNA and proteins of pathogens. ROS are able to interact with the voltage-dependent Na^+ channels, and maintain the channels in an open state for longer and cause membrane depolarization [19]. The disruption of the mitochondrial membrane potential caused by ROS therefore promotes the release of cytochrome c into the cytosol, which leads to the aggregation of the adaptor molecule apoptotic protease-activating factor 1, and the initiation of apoptosis.

In the present study, aconitine was applied to two types of hepatic carcinoma cells, HepG2 and Huh7, and the normal hepatic cell line L02 at various concentrations, and it was found that aconitine specifically inhibits the proliferation of the cancer cells in a dose-dependent manner. Further study found that aconitine induced apoptosis by activating the production of ROS, leading to an increased release of cytochrome *c* from mitochondria and enhanced apoptosis. An i*n vivo* investigation also determined that aconitine was able to inhibit the growth of tumors in mice. These results suggest that aconitine has the potential to be developed into an effective anti-HCC agent.

Materials and methods

Cell culture and reagents

HepG2 and Huh7 human hepatocellular carcinoma cells and L02 human hepatic cells (Shanghai Institute of Cell Biology, Chinese Academy of Sciences, Shanghai, China) were cultured in complete Dulbecco's modified Eagle's medium (C-DMEM; Mediatech Inc.; Corning Incorporated, Corning, NY, USA) containing 10% heat-inactivated fetal bovine serum (FBS; Sigma-Aldrich; Merck KGaA, Darmstadt, Germany), 1% penicillin and streptomycin (Lonza Group, Ltd., Basel, Switzerland) in a 37°C incubator containing 5% CO_2. The aconitine was purchased from Sigma-Aldrich; Merck KGaA and its purity was >95%, as confirmed using high-performance liquid chromatography (HPLC) by Sigma-Aldrich (Merck-KGaA). It was dissolved in C-DMEM at a concentration of 654 mg/ml as a stock solution. The aconitine stock solution was freshly diluted in C-DMEM containing 10% FBS prior to use in each experiment.

Cell viability assay

HepG2 cells were plated at a density of 1×10^4 cells/well in a 96-well plate. After 24 h, the cells were mock-treated or treated with aconitine at various concentrations (between 0 and 100 μg/ml) for 24, 48 and 72 h. The cell viability was determined using an MTT assay, and the absorbance was measured at 570 nm using a plate reader (SpectraMax; Molecular Devices, Sunnyvale, CA, USA). The results were collated from three individual experiments.

Apoptosis assay

Annexin V-fluorescein isothiocyanate (FITC)/propidium iodide (PI) double staining was employed to quantify the apoptosis of HepG2 cells treated with either aconitine or with the

caspase inhibitor benzyloxycarbonyl-Val-Ala-Asp-fluoromethylketone (Z-VAD-FMK). Following the treatment of cells with aconitine at the indicated concentrations for 72 h, the cells were harvested and washed twice with ice-cold PBS, and then stained using an annexin V-FITC/PI double fluorescence apoptosis detection kit (Roche Diagnostics GmbH, Mannheim, Germany), according to the manufacturer's protocol. The samples were analyzed using a FACSCalibur flow cytometer (BD Biosciences, Franklin Lakes, NJ, USA) within 1 h of staining. The results were analyzed using Cell Quest software (version 6.0; BD Biosciences).

Western blot analysis

HepG2 cells with or without aconitine treatment were harvested and lysed on ice in a solubilizing buffer [300 mM NaCl, 50 mM Tris-HCl, pH 7.6, 0.5 % Triton X-100, 2 mM phenylmethane sulfonyl fluoride (PMSF), 2 µl/ml aprotinin and 2 µl/ml leupeptin], supplemented with a protein kinase inhibitor cocktail (complete™ Mini EDTA-free; Sigma-Aldrich; Merck KGaA). Following centrifugation at 10,000× g for 10 mins, the supernatants were collected. Total protein levels of the cell lysates were quantified using a bicinchoninic acid protein assay kit (Pierce; Thermo Fisher Scientific, Inc., Waltham, MA, USA), according to the manufacturer's protocol. Protein (40 ìg/lane) was separated on 10% gradient polyacrylamide gels and transferred onto polyvinylidene difluoride membranes. The membranes were blotted with antibodies against poly (ADP-ribose) polymerase (PARP) (catalog no. 9542S; Cell Signaling Technology, Inc., Danvers, MA, USA), B-cell lymphoma 2 (Bcl-2; catalog no. ab32124; Abcam, Cambridge, MA, USA), Bcl-2-associated X protein (Bax; catalog no. ab53154; Abcam), cleaved caspase 3 (catalog no. ab32351; Abcam), cytochrome *c* (catalog no. 4272S; Cell Signaling Technology, Inc.), GAPDH (catalog no. ab8245; Abcam), tubulin (catalog no. 2146S; Cell Signaling Technology, Inc.) and cytochrome oxidase subunit IV (Cox IV; catalog no. 4850S; Cell Signaling Technology, Inc.) at the dilutions recommended by the manufacturers in a blocking solution (5% skim milk diluted in Tris-Buffered Saline Tween) overnight at 4°C, and then incubated for 2 h with a horseradish peroxidase-conjugated secondary antibody (1:2,000-1:5,000; catalog no. 7074; Cell Signaling Technology, Inc.) at room temperature. The signals were visualized using an enhanced chemiluminescence detection system (GE Healthcare, Chicago, IL, USA). GAPDH, tubulin or Cox IV was blotted as a loading control. ImageJ (version v2.1.4.7; National Institutes of Health, Bethesda, MD, USA) was used for the densitometric analysis of bands.

Collection of cytosol and mitochondrial proteins

HepG2 cells (5×10^6 cells/ml) were harvested by centrifugation at 1,000× g for 10 min, washed twice with PBS and resuspended in lysis buffer A (250 mM sucrose, 10 mM KCl, 1.5 mM $MgCl_2$, 1 mM EDTA, 1 mM EGTA, 0.5 mM dithiothreitol, 0.1 mM PMSF, 10 µg/ml aprotinin, 10 µg/ml leupeptin and 20 mM HEPES-KOH, pH 7.5). The cell lysates were further homogenized by successive passages through a 26-gauge hypodermic needle. The homogenates were centrifuged at 100,000× g for 15 min, and the supernatant was used for western blot analysis.

Mitochondrial fractions were isolated using the digitonin lysis method [20]. Briefly, cells (5×10^6) were incubated with an ice-cold digitonin lysis buffer (250 mM sucrose, 10 mM KCl, 1.5 mM $MgCl_2$, 1 mM EDTA, 1 mM EGTA, 0.5 mM dithiothreitol, 0.1 mM PMSF, 190 µg/ml digitonin and 20 mM HEPES-KOH, pH 7.5) for 10 min. The cell suspension was centrifuged at 2,500× g for 10 min, and the supernatant was centrifuged again at 15,000× g for 15 min. The pellet (mitochondrial fraction) was resuspended in buffer B (10 mM Tris-HCl, pH 7.4, 150 mM NaCl, 5 mM EDTA, 0.5% Triton X-100, 10 µg/ml aprotinin, 1 mM PMSF and 1 mM sodium orthovanadate) for 30 min on ice. The suspension was centrifuged at 12,000× g for 30 min at 4°C in a microcentrifuge, and the supernatant was collected as the mitochondrial protein extract.

Measurement of ROS

The intracellular changes in ROS generation were measured by staining the HepG2 cells with 2',7'-dichlorodihydrofluoresceindiacetate (DCFH-DA) (Sigma-Aldrich; Merck KGaA). The cell membrane-permeant fluorescent dye DCFH-DA is converted into cell membrane-impermeant non-fluorescent compound 2',7'-dichlorodihydrofluorescein (DCFH) by intracel-

lular esterases. The oxidation of DCFH by ROS produces fluorescent 2',7'-dichlorofluorescein (DCF). The fluorescence intensity of DCF inside the cells is proportional to the amount of peroxide produced. After 72 h of treatment with 25 and 50 μg/ml aconitine, the HepG2 cells were further incubated with 10 μM DCFH-DA (diluted with free FBS DMEM) at 37°C for 30 min in the dark. The cells were harvested, washed, resuspended in PBS, filtered with 300 aperture filters, and the DCF fluorescence was analyzed using flow cytometry (BD LSRII flowcytometer; BD Biosciences). The excitation wavelength was 488 nm, and the emission wavelength was 530 nm. 10000 cells in every group were acquired. The results were analyzed using CellQuest software (version 6.0; BD Biosciences).

Measurement of the mitochondrial membrane potential

The mitochondrial membrane potential was determined using the 5,5',6,6'-tetrachloro-1,1',3,3'-tetraethylbenzimidazolylcarbocyanine iodide (JC-1) probe (Beyotime Institute of Biotechnology, Haimen, China) as described previously [21, 22]. JC-1 is used to monitor mitochondrial membrane depolarization. In healthy cells with a high mitochondrial membrane potential, JC-1 spontaneously forms complexes known as J-aggregates with an intense red fluorescence. Conversely, in apoptotic or unhealthy cells with low mitochondrial membrane potential, JC-1 remains in the monomeric form, which exhibits only green fluorescence. Thus, mitochondrial depolarization is indicated by an increase in the green/red fluorescence intensity ratio. Briefly, following treatment of HepG2 cells with 25 and 50 μg/ml aconitine for 72 h, the cells were suspended in a culture medium to a concentration of 1×10^5 cells/ml and incubated with 20 nM JC-1 at 37°C in the dark for 30 min. Next, the cells were washed twice with the JC-1 staining buffer, and the fluorescence intensity of the JC-1 aggregates was detected at an excitation wavelength of 525 nm and an emission wavelength of 590 nm. The JC-1 monomer was measured at an excitation wavelength of 490 nm and an emission wavelength of 530 nm using a fluorescence microplate reader (BD Biosciences). The fluorescence intensity ratio of monomers to monomers plus aggregates was calculated as an indicator of the proportion of depolarized cells.

Mouse xenografting

A total of 30 6-week-old male BALB/c nude mice (weight, ~20 g) were purchased from the Institute of Animal Center, Chinese Academy of Science (Shanghai, China). The mice had free access to standard animal food and water throughout the experiment. Their housing conditions included 12 h light/dark cycles, the air was ventilated 15 times every hour, and the temperature was maintained between 20 and 22°C. All animal studies were conducted in accordance with an animal use protocol that was approved by the Animal Care and Use Committee of the Second Military Medical University. Huh7 cells (6×10^5) in 0.1 ml PBS were injected subcutaneously into the right flank of each of the fifteen BALB/c nude mice. At 14 days after inoculation, the subcutaneous nodules reached ~5 mm in diameter. The mice were then randomly assigned to three groups (5 in each group): Group 1, PBS; Group 2, aconitine (2 mg/kg); and Group 3, aconitine (4 mg/kg). Tumor volumes (Vt) were measured once every 3 days for 3 weeks, using a vernier caliper, and subsequently calculated using the following formula: 0.5 × height × length × width. All the mice were sacrificed 21 days following treatment by CO_2 asphyxiation (The device is filled with 100% CO_2 within about 5 mins). Another set of male 15 BALB/C nude mice aged 4-6 weeks (weight, ~20 g) was used to observe the survival time. These 15 mice were injected with Huh7 cells, divided into three groups, and treated with different treatments. All of the operations were the same as the first set of 15 mice. The survival time of the mice due to the heavy tumor burden was observed until the experiments were terminated.

Histology and immunohistochemistry

All excised tumors were fixed in 10% neutral formaldehyde for 6 h at room temperature and embedded with paraffin. Tumor sections (4 ìm) were subjected to hematoxylin (0.5%) and eoisin (1%) staining for 5 min in 22°C and immunohistochemistry.

The sections were blocked with 0.2% bovine serum album (catalog no. 15019; Cell Signaling Technology, Inc.) at 37°C 10 min, and incubat-

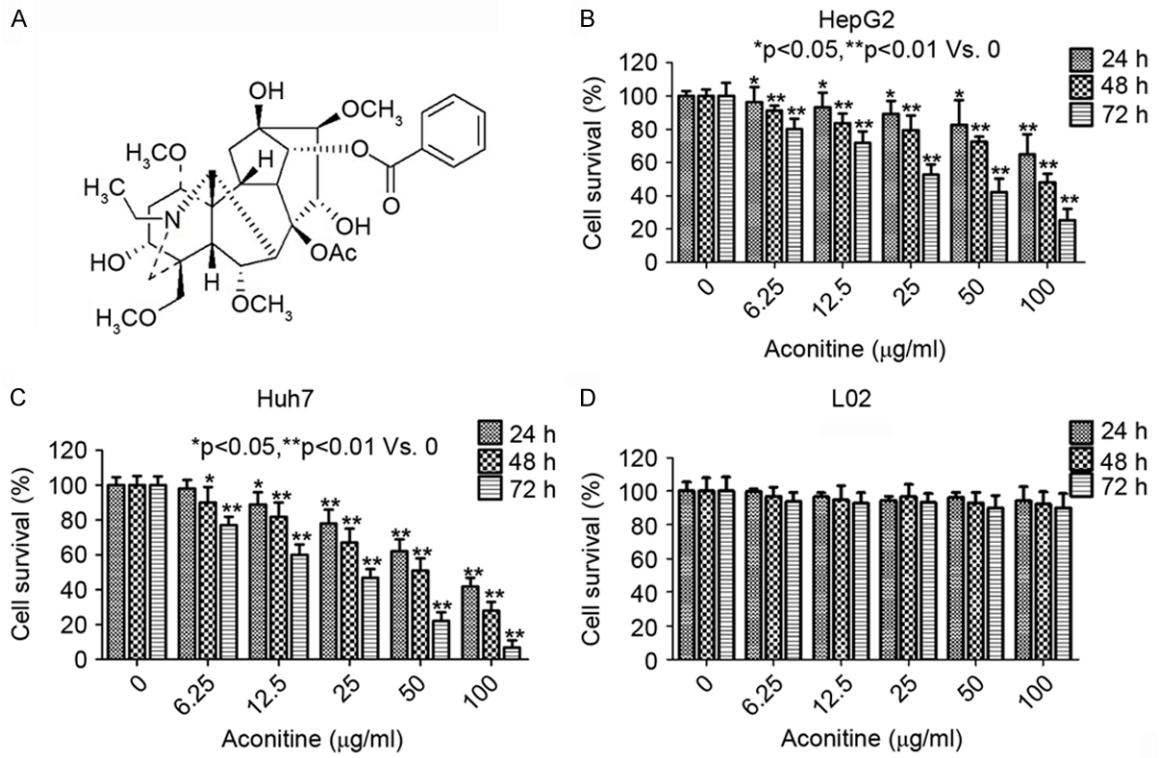

Figure 1. Aconitine inhibits the viability of hepatocellular carcinoma cells, but not normal hepatic cells. (A) Chemical structure of aconitine. (B) HepG2, (C) Huh7 and (D) L02 cells were treated with aconitine at various concentrations for 24, 48 or 72 h. Cell survival was determined using an MTT assay. Results are from three independent experiments, each conducted in triplicate.

ed with the anti-human Ki-67 antibody (catalog no. 9449T, 1:1500, Cell Signaling Technology, Inc.) at 4°C overnight. Then, redundant antibodies were washed and the second antibody with horseradish peroxidase (catalog no. 8125, 1:2000, Cell Signaling Technology, Inc.) was used for 30 min incubation at 37°C. Finally, the avidin-biotin horseradish peroxidase system was used to develop sections with diaminobenzidine (DAB, catalog no. 8059, Cell Signaling Technology, Inc.). The results were observed by light microscope (BX51, Olympus America, Inc.) with the magnification of 200×, and photographed with a digital camera (DP70, Olympus America, Inc.).

The expression of Ki-67 was evaluated through immunohistochemistry using the mouse anti-human Ki-67 antibody (catalog no. 9449T, Cell Signaling Technology, Inc.).

Statistical analysis

Statistical analysis was performed using SPSS software (version 20.0; IBM Corp., Armonk, NY, USA). The data were expressed as the mean ± standard deviation. Significant differences between groups were analyzed by one-way factorial analysis of variance or Student's t test. $P<0.05$ was considered to indicate a statistically significant difference.

Results

Aconitine inhibits the viability of HCC cells, but not normal hepatic cells

Since aconitine, the structure of which is presented in **Figure 1A**, has been demonstrated to inhibit the viability of breast cancer and melanoma cells, the aim of the present study was to determine whether it has the same effect on HCC cells. For this purpose, hepatic carcinoma HepG2 and Huh7 cells were treated with aconitine at concentrations of 0, 6.25, 12.5, 25, 50 and 100 μg/ml. Normal hepatic L02 cells were also included as a negative control. The viability of the cells was determined using an MTT assay at 24, 48 and 72 h after treatment. As presented in **Figure 1**, at 24, 48 and 72 h after treat-

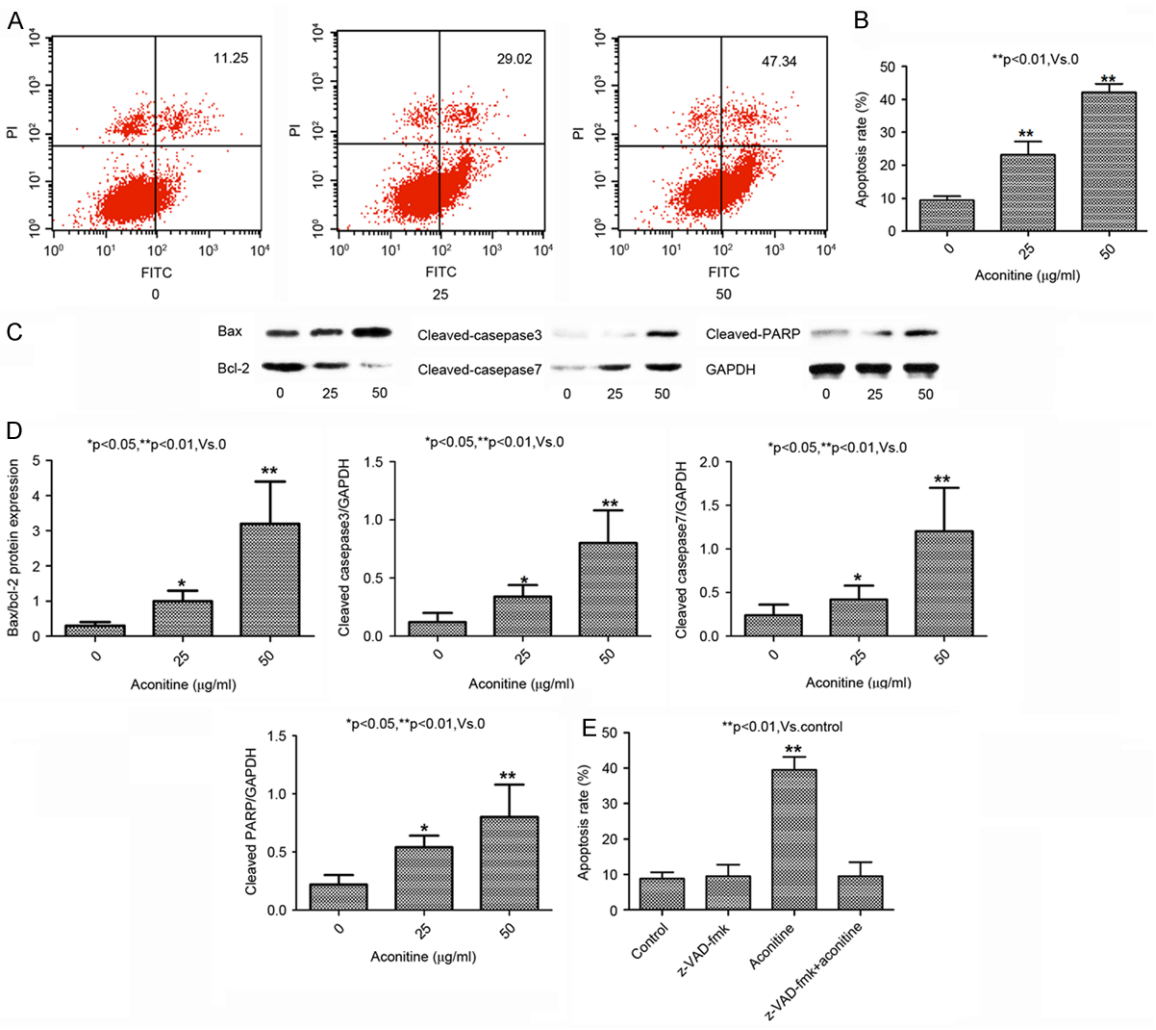

Figure 2. Aconitine induces apoptosis in HepG2 cells. (A) Representative flow cytometric analysis of HepG2 cells stained with annexin V-FITC/PI following exposure to 0 (left panel), 25 (middle panel) and 50 (right panel) μg/ml aconitine for 72 h. The number in the top-right corner of each panel indicates the percentage of cells undergoing apoptosis. (B) The proportion of cells undergoing apoptosis following treatment with aconitine at various concentrations. (C) HepG2 cell lysates treated with aconitine at concentrations of 0, 25 and 50 μg/ml were immunoblotted for Bax, Bcl-2, cleaved caspase 3, cleaved caspase 7 and cleaved PARP. GAPDH was used as a loading control. (D) Densitometric analysis of the Western blot bands in (C) using ImageJ software. (E) Aconitine induced apoptosis in HepG2 cells, but Z-VAD-FMK inhibited the apoptosis in the presence of 50 μg/ml aconitine. FITC, fluorescein isothiocyanate; PI, propidium iodide; Bax, Bcl-2-associated X protein; Bcl-2, B-cell lymphoma 2; PARP, poly (ADP-ribose) polymerase; Z-VAD-FMK, benzyloxycarbonyl-Val-Ala-Asp-fluoromethylketone.

ment, higher concentrations of aconitine produced a significant inhibitory effect on the viability of HepG2 (**Figure 1B**) and Huh7 (**Figure 1C**) cells. However, even at a concentration of 100 μg/ml, aconitine had little effect on the viability of the L02 cells (**Figure 1D**). Conversely, at a certain concentration, the longer treatment led to a significant inhibition of the viability of the tumor cells (**Figure 1B**, **1C**). These results suggest that aconitine inhibits the viability of HCC cells in a time- and dose-dependent manner. This inhibition appeared to be specific to carcinoma cells, as the viability of normal hepatic cells was barely affected by the drug.

Aconitine inhibits the viability of HCC cells by inducing apoptosis

Since aconitine is inhibitory to HCC cells, the next step was to elucidate the underlying molecular mechanism of how aconitine may regulate the viability of the cancer cells. It was speculated that this inhibition was achieved by

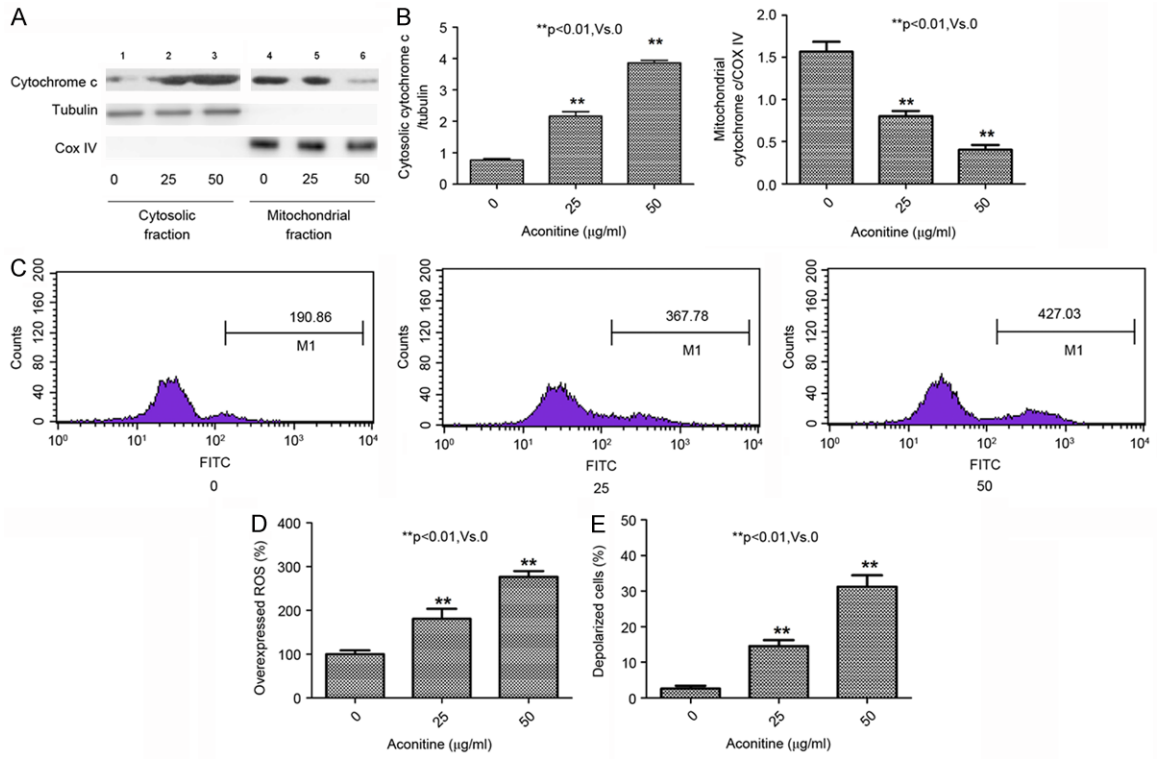

Figure 3. Aconitine induces the release of cytochrome *c* from mitochondria and the increase in the intracellular ROS level in HepG2 cells. A. Aconitine induced the release of cytochrome *c* to the cytosol in HepG2 cells treated with 25 (lane 2) and 50 (lane 3) μg/ml aconitine. Lanes 1 and 4 are solvent controls. Lanes 5 and 6 indicate the decrease in mitochondrial cytochrome *c* when cells were treated with 25 and 50 μg/ml aconitine, respectively. B. Densitometric analysis of the Western blot bands, presented as cytosolic cytochrome *c*/tubulin (left panel) and mitochondrial cytochrome *c*/Cox IV (right panel) ratios. C. The proportion of depolarized cells following treatment with aconitine at various concentrations. The fluorescence intensity ratio of monomers to monomers plus aggregates was determined as an indicator of the proportion of depolarized cells. D. Detection of intracellular ROS production in HepG2 cells treated with solvent (left panel), 25 (middle panel) and 50 (right panel) μg/ml aconitine. Cells were stained with 2',7'-dichlorodihydrofluorescein diacetate. E. The expression of ROS in cells treated with aconitine at various concentrations. Results are the mean ± standard deviation of three independent experiments. ROS, reactive oxygen species; COX IV, cytochrome oxidase subunit IV; FITC, fluorescein isothiocyanate.

activating the apoptosis pathway within the cells. To test this hypothesis, HepG2 cells were stained with annexin V-FITC/PI following treatment of the cells with 25 and 50 μg/ml aconitine for 72 h, and then comparing the results with those from the negative control cells treated with C-DMEM containing 10% FBS only. Representative flow cytometric data for the cells treated with solvent, 25 and 50 μg/ml aconitine are presented in **Figure 2A**. The increase in the proportion of cells undergoing apoptosis was found to be associated with the increase in the aconitine concentration used to treat the cells (**Figure 2B**).

To further characterize these cells, the lysates of the HepG2 cells were immunoblotted with apoptotic markers, including Bax, Bcl-2, cleaved caspases 3 and 7, and cleaved PARP, as well as GAPDH as a loading control. As presented in **Figure 2C**, the levels of Bax, cleaved caspases 3 and 7, and cleaved PARP increased, but the level of the anti-apoptotic protein Bcl-2 decreased in an aconitine dose-dependent manner. The level of GAPDH remained largely unchanged. The increased Bax/Bcl-2 ratio was determined following a densitometric analysis of the Western blot bands (**Figure 2D**) indicating the activation of apoptosis. To confirm that the induction of apoptosis was the main cause of the inhibition of the viability of the cancer cells, the caspase inhibitor Z-VAD-FMK was added together with aconitine to the HepG2 cells, and it was identified that the percentage of cells undergoing apoptosis was decreased to a level similar to that in the control cells (**Figure**

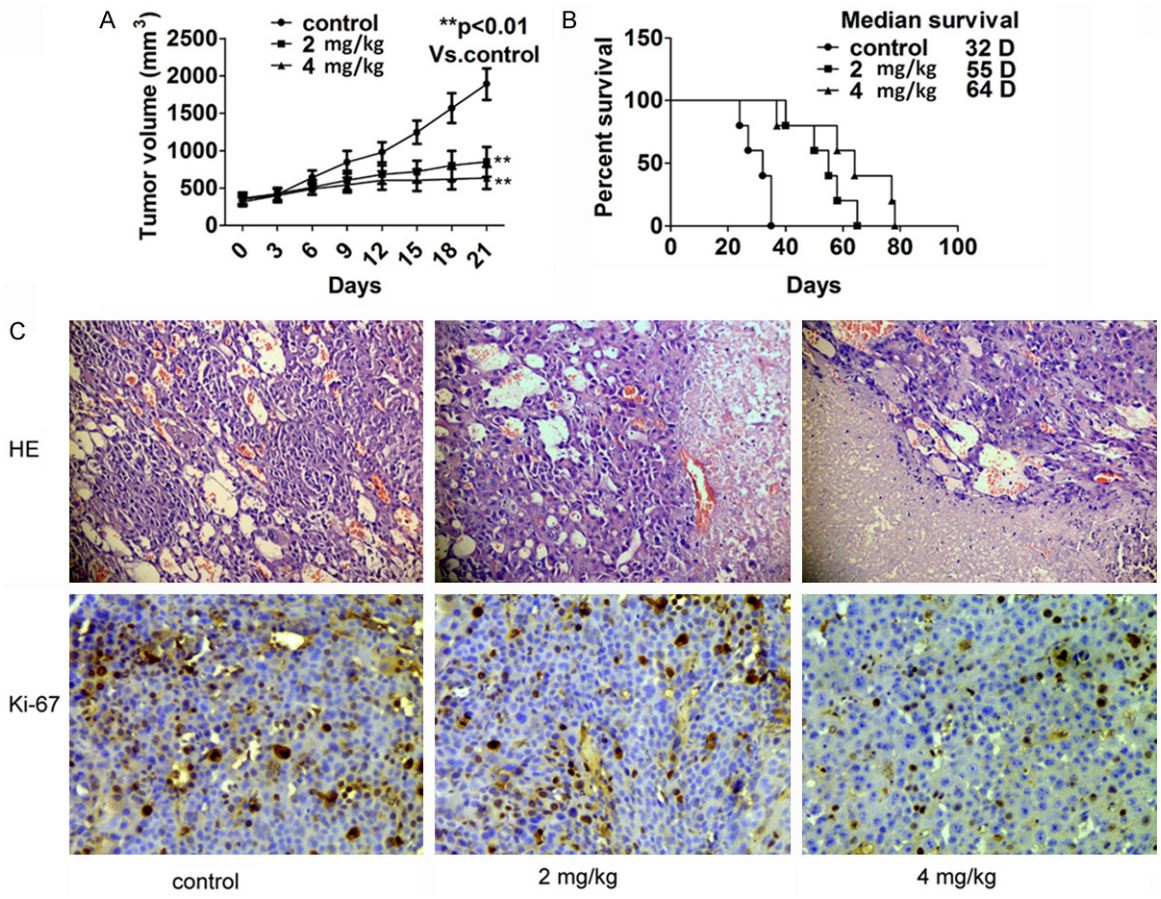

Figure 4. Aconitine inhibits the growth of tumors *in vivo*. A. Tumor growth was inhibited by the injection of aconitine into the tumor in mice. B. Aconitine extended the survival time of mice. C. HE staining (upper panel) and Ki-67 staining (lower panel) of tumor tissue sections from mice injected with solvent and aconitine at concentrations of 2 and 4 mg/kg. HE, hematoxylin and eosin; D. Days.

2E). It was noted that the addition of Z-VAD-FMK alone did not have any effect on the cells. These results suggest that aconitine specifically inhibits the viability of human HCC cells by inducing apoptosis.

Aconitine induces apoptosis possibly by increasing the production of ROS and promoting the release of cytochrome c from mitochondria

There are two main mechanisms that regulate apoptosis: Targeting mitochondria functionality or transducing apoptotic signals via adaptor proteins on the membrane. Since changes in cleaved PARP, cleaved caspases 3 and 7, Bcl-2 and Bax were detected in the HepG2 cells, it was hypothesized that mitochondria were involved in the aconitine-induced apoptosis. To test this hypothesis, HepG2 cells were treated with solvent or aconitine at concentrations of 25 and 50 μg/ml for 72 h, and cytochrome *c* was immunoblotted in the cytosol and mitochondria. It was found that, in association with the increase in aconitine concentration, the level of cytochrome *c* increased in the cytosol and decreased in the mitochondria in an aconitine dose-dependent manner, whereas the level of tubulin in the cytosolic fractions and the level of Cox IV in the mitochondrial fractions remained unaltered (**Figure 3A**). The densitometric analysis of the level changes of cytosolic and mitochondrial cytochrome *c* relative to the level of tubulin is presented in **Figure 3B**. This result suggests that aconitine induces apoptosis through the mitochondrial signaling pathway.

The release of cytochrome *c* into the cytosol is often caused by a loss of potential in the mitochondrial membrane [23]. To investigate whether the mitochondrial membrane became depolarized following aconitine treatment, the

HepG2 cells were stained with JC-1 dye and their fluorescence intensity was determined. As presented in **Figure 3C**, the proportion of depolarized cells increased in an aconitine dose-dependent manner. The depolarization of the mitochondrial membrane may be induced by ROS, and, if the intracellular ROS level reaches a certain high level, ROS becomes toxic and selectively kills cancer cells by promoting apoptosis. To ascertain whether aconitine also regulates the ROS level, the intracellular ROS production was determined. **Figure 3D** presents the results of the analysis of intracellular ROS production in HepG2 cells treated with solvent, 25 and 50 μg/ml aconitine for 72 h. The results presented in **Figure 3E** indicate that aconitine led to an increase in the ROS level in a dose-dependent manner in the HepG2 cells. These results suggest that aconitine may promote apoptosis in HepG2 cells by inducing the production of intracellular ROS, which, in turn, triggers the depolarization of the mitochondrial membrane and therefore leads to the release of cytochrome *c* from the mitochondria into the cytosol.

Aconitine inhibits tumor growth in vivo

Considering that aconitine inhibits the viability of HepG2 cells, we investigated whether it was also able to inhibit the growth of tumors *in vivo*. For this purpose, nude mice were xenografted with Huh7 cells and the tumor was allowed to grow to ~5 mm in diameter. Then, solvent or aconitine was injected into the tumors, and the size of the tumor was measured every 3 days until 21 days after the injection. Results presented in **Figure 4A** indicate that aconitine significantly decreased the proliferation rate of the tumor in volume, and the injection of aconitine at 4 mg/kg almost completely inhibited the growth of the tumor. It was also demonstrated that aconitine extended the survival time of the mice. At the injection amount of 4 mg/kg, aconitine doubled the survival time of the mice compared with the mice in the solvent control (**Figure 4B**). To examine the histology of the tumors and the proliferation of tumor cells, tumor tissue sections were stained with hematoxylin and eosin (**Figure 4C**, upper panel) and Ki-67 (**Figure 4C**, lower panel). Along with the increase in the amount of aconitine being injected, the staining by HE and Ki-67 decreased in the tumor tissue sections, indicating a deceleration in tumor cell proliferation.

Discussion

In the present study, it was demonstrated that aconitine, a constituent from *Aconitum* plant extracts, has an inhibitory effect on HCC cell viability *in vitro* and *in vivo*. This inhibition is achieved by inducing apoptosis, possibly by increasing the production of ROS and, therefore, promoting the release of cytochrome *c* from mitochondria. Aconitine inhibited the proliferation of two HCC cell lines, HepG2 and Huh7, in a dose- and time-dependent manner, where increased doses and longer treatment resulted in more marked inhibition of the proliferation of these carcinoma cells. Furthermore, the same conditions exhibited little effect on normal hepatic L02 cells, suggesting that the inhibition is specific towards the carcinoma cells.

A previous study demonstrated that aconitine was able to induce apoptosis in melanoma cells, and it was hypothesized that the same mechanism also applied to HCC cells [16]. To test this hypothesis, HepG2 cells were stained with annexin V-FITC/PI, and it was identified that the proportion of apoptotic cells increased in the aconitine-treated samples. The increase in the proportion of apoptotic cells was positively associated with the length of treatment and the dose of aconitine being applied, indicating that aconitine was the agent that induced apoptosis. Furthermore, when the pan-caspase inhibitor Z-VAD-FMK was added together with aconitine (50 μg/ml), the apoptotic rate was decreased to a level similar to that of the control cells. Importantly, the inhibitor alone had little effect on the cell apoptotic rate compared with the control cells, indicating that the decrease in the apoptotic rate in cells treated with the combination of aconitine and inhibitor was due to the inhibition of apoptosis. This result suggests that apoptosis in HepG2 cells was induced by aconitine. Notably, the ability of aconitine to induce apoptosis appears to be specific to cancer cells, as the addition of aconitine did not affect the viability of normal hepatic L02 cells.

Following aconitine treatment, changes in cleaved PARP, caspases 3 and 7, Bcl-2 and Bax were detected in HepG2 cells characteristic of mitochondria-regulated apoptosis. This result prompted the investigation of the role of mitochondria in aconitine-induced apoptosis.

Cytochrome *c* was immunoblotted in the cytosolic and mitochondrial samples, and it was identified that aconitine treatment led to the increase in cytochrome *c* in the cytosol and the decrease in cytochrome *c* in the mitochondria. It has been reported that oxidation of the mitochondrial pores by ROS may contribute to cytochrome *c* release due to the disruption of the mitochondrial membrane potential. The release of cytochrome *c* from mitochondria is therefore possibly due to the depolarization of the mitochondrial membrane. To verify this, the production of intracellular ROS was examined in HepG2 cells. It was demonstrated that the treatment with aconitine led to the increase in the ROS level associated with the increase in the dose of aconitine being applied to the HepG2 cells. It is currently unclear how the initial ROS is produced. Intracellular ROS are typically produced through multiple mechanisms depending on the cell and tissue types. The majority of ROS comes from cell membranes, mitochondria, peroxisomes and the endoplasmic reticulum [24]. Thus, it is possible that mitochondria are the source and the target of ROS in this case. The results suggest that aconitine may cause the increase in the intracellular ROS level, which triggers the depolarization of the mitochondrial membrane and the enrichment of cytosolic cytochrome *c*, leading to the induction of apoptosis in HepG2 cells.

ROS are a 'double-edged sword'. On one hand, ROS facilitate cancer cell survival when at low levels, and, on the other, are able to suppress tumor growth through the sustained activation of cell-cycle inhibitors [25-27] and the induction of apoptosis at high concentrations. Cancer cells typically exhibit increased ROS levels and depend heavily on the antioxidant defense system. ROS-increasing drugs including aconitine further increase the cellular ROS stress level, resulting in an overall increase in endogenous ROS, which, when above a cellular tolerance threshold, may induce cell death. In the present study, the ROS level was increased between 2- and 3-fold in cells treated with aconitine compared with the levels in the control cells, therefore possibly reaching a level that was inhibitory to cancer cells. However, under lower basal stress and production from normal metabolism, normal cells may have an increased capacity to withstand additional ROS than do cancer cells [28]. This may explain why aconitine preferentially induced apoptosis in HCC cells, but not in normal L02 cells. Although preliminary, our results also demonstrated that, at relatively high concentrations, aconitine was able to inhibit the growth of tumors *in vivo*.

Wutou, a traditional Chinese herb, has been successfully used to treat HCC in a number of hospitals, including our hospital, the Changhai Hospital (Shanghai, China) [29, 30]. *In vitro* study has demonstrated that aconitine, the main constituent of Wutou, induced apoptosis in HCC cells, but not in normal hepatic cells. This was possibly due to the increased production of ROS, which subsequently caused the depolarization of the mitochondrial membrane and the release of cytochrome *c* into the cytosol. An i*n vivo* study demonstrated that aconitine was able to significantly inhibit the growth of tumors in a mouse model. It is noteworthy that, in the present study, aconitine only became effective at concentrations of 25 and 50 μg/ml *in vitro*, and 2 mg/kg and 4 mg/kg *in vivo*. The requirement for a relatively high dose of aconitine to achieve inhibition of cancer cells *in vitro* and tumors *in vivo* suggests that other factors in Wutou may also contribute to the anticancer effect, or that aconitine and other factors work synergistically to inhibit the proliferation of cancer cells. This requires further investigation. Nevertheless, the results of the present study suggest that aconitine has the potential to be developed into an effective anticancer drug to treat patients with HCC.

Acknowledgements

The present study was supported in part by the National Natural Science Foundation of China (grant number: 81774244 to LW; 81303112 to LW; 81403385 to XL) and the Natural Science Foundation of Shanghai (grant number: 12ZR1437400 to LW).

Disclosure of conflict of interest

None.

Address correspondence to: Lina Wang and Xia Li, Department of Traditional Chinese Medicine, Changhai Hospital, Naval Medical University, No. 168 Changhai Road, Shanghai 200433, PR China. E-mail: rena1022@163.com (LNW); 13364317179@163.com (XL)

References

[1] Bertuccio P, Turati F, Carioli G, Rodriguez T, La Vecchia C, Malvezzi M and Negri E. Global trends and predictions in hepatocellular carcinoma mortality. J Hepatol 2017; 67: 302-309.

[2] Ferlay J, Soerjomataram I, Dikshit R, Eser S, Mathers C, Rebelo M, Parkin DM, Forman D and Bray F. Cancer incidence and mortality worldwide: sources, methods and major patterns in GLOBOCAN 2012. Int J Cancer 2015; 136: E359-386.

[3] Germano D and Daniele B. Systemic therapy of hepatocellular carcinoma: current status and future perspectives. World J Gastroenterol 2014; 20: 3087-3099.

[4] Ling CQ, Wang LN, Wang Y, Zhang YH, Yin ZF, Wang M and Ling C. The roles of traditional Chinese medicine in gene therapy. J Integr Med 2014; 12: 67-75.

[5] Ling CQ, Yue XQ and Ling C. Three advantages of using traditional Chinese medicine to prevent and treat tumor. J Integr Med 2014; 12: 331-335.

[6] Maida M, Iavarone M, Raineri M, Cammà C and Cabibbo G. Second line systemic therapies for hepatocellular carcinoma: reasons for the failure. World J Hepatol 2015; 7: 2053-2057.

[7] Suzuki T, Miyamoto K, Yokoyama N, Sugi M, Kagioka A, Kitao Y, Adachi T, Ohsawa M, Mizukami H and Makino T. Processed aconite root and its active ingredient neoline may alleviate oxaliplatin-induced peripheral neuropathic pain. J Ethnopharmacol 2016; 186: 44-52.

[8] Wang XL, Ma F and Wu XZ. Anticancer effects of 5-fluorouracil combined with warming and relieving cold phlegm formula on human breast cancer. Chin J Integr Med 2012; 18: 599-604.

[9] Ji XM, Wu ZC, Liu GW, Yu HY, Liu H, Wang ZT, Wei XH and Ouyang B. Wenxia Changfu formula induces apoptosis of lung adenocarcinoma in a transplanted tumor model of drug-resistance nude mice. Chin J Integr Med 2016; 22: 752-758.

[10] Chen D, Cao R, He J, Guo Y, Wang L, Ji W and Wu X. Synergetic effects of aqueous extracts of fuzi (radix aconiti lateralis preparata) and tubeimu (rhizoma bolbostemmatis) on MDA-MB-231 and SKBR3 cells. J Tradit Chin Med 2016; 36: 113-124.

[11] Sheng LH, Xu M, Xu LQ and Xiong F. [Cytotoxic effect of lappaconitine on non-small cell lung cancer in vitro and its molecular mechanism]. Zhong Yao Cai 2014; 37: 840-843.

[12] Yin TP, Cai L, He JM, Dong JW, Fang HX, Zhou H and Ding ZT. Three new diterpenoid alkaloids from the roots of aconitum duclouxii. J Asian Nat Prod Res 2014; 16: 345-350.

[13] Pyaskovskaya ON, Boychuk IV, Fedorchuk AG, Kolesnik DL, Dasyukevich OI and Solyanik GI. Aconitine-containing agent enhances antitumor activity of dichloroacetate against Ehrlich carcinoma. Exp Oncol 2015; 37: 192-196.

[14] Li Y, Gao F, Zhang JF and Zhou XL. Four new diterpenoid alkaloids from the roots of aconitum carmichaelii. Chem Biodivers 2018; 15: e1800147.

[15] Guo BF, Liu S, Ye YY and Han XH. Inhibitory effects of osthole, psoralen and aconitine on invasive activities of breast cancer MDA-MB-231BO cell line and the mechanisms. Zhong Xi Yi Jie He Xue Bao 2011; 9: 1110-1117.

[16] Du J, Lu X, Long Z, Zhang Z, Zhu X, Yang Y and Xu J. In vitro and in vivo anticancer activity of aconitine on melanoma cell line B16. Molecules 2013; 18: 757-767.

[17] Tai CJ, El-Shazly M, Wu TY, Lee KT, Csupor D, Hohmann J, Chang FR and Wu YC. Clinical aspects of aconitum preparations. Planta Med 2015; 81: 1017-1028.

[18] Ginter E, Simko V and Panakova V. Antioxidants in health and disease. Bratisl Lek Listy 2014; 115: 603-606.

[19] Borcsa B, Fodor L, Csupor D, Forgo P, Molnár A and Hohmann J. Diterpene alkaloids from the roots of aconitum moldavicum and assessment of Nav 1.2 sodium channel activity of aconitum alkaloids. Planta Med 2014; 80: 231-236.

[20] Dai Y, Liu M, Tang W, Li Y, Lian J, Lawrence TS and Xu L. A smac-mimetic sensitizes prostate cancer cells to TRAIL-induced apoptosis via modulating both IAPs and NF-kappaB. BMC Cancer 2009; 9: 392.

[21] Lv W, Sheng X, Chen T, Xu Q and Xie X. Jaceosidin induces apoptosis in human ovary cancer cells through mitochondrial pathway. J Biomed Biotechnol 2008; 2008: 394802.

[22] Ling X, Zhou Y, Li SW, Yan B and Wen L. Modulation of mitochondrial permeability transition pore affects multidrug resistance in human hepatocellular carcinoma cells. Int J Biol Sci 2010; 6: 773-783.

[23] Mondal J, Das J, Shah R and Khuda-Bukhsh AR. A homeopathic nosode, hepatitis C 30 demonstrates anticancer effect against liver cancer cells in vitro by modulating telomerase and topoisomerase II activities as also by promoting apoptosis via intrinsic mitochondrial pathway. J Integr Med 2016; 14: 209-218.

[24] Shi Y, Pulliam DA, Liu Y, Hamilton RT, Jernigan AL, Bhattacharya A, Sloane LB, Qi W, Chaudhuri A, Buffenstein R, Ungvari Z, Austad SN and Van Remmen H. Reduced mitochondrial ROS, enhanced antioxidant defense, and distinct

age-related changes in oxidative damage in muscles of long-lived Peromyscus leucopus. Am J Physiol Regul Integr Comp Physiol 2013; 304: R343-355.

[25] Ramsey MR and Sharpless NE. ROS as a tumour suppressor? Nat Cell Biol 2006; 8: 1213-1215.

[26] Takahashi A, Ohtani N, Yamakoshi K, Iida S, Tahara H, Nakayama K, Nakayama KI, Ide T, Saya H and Hara E. Mitogenic signalling and the p16INK4a-Rb pathway cooperate to enforce irreversible cellular senescence. Nat Cell Biol 2006; 8: 1291-1297.

[27] Zang QQ, Zhang L, Gao N and Huang C. Ophiopogonin D inhibits cell proliferation, causes cell cycle arrest at G2/M, and induces apoptosis in human breast carcinoma MCF-7 cells. J Integr Med 2016; 14: 51-59.

[28] Trachootham D, Alexandre J and Huang P. Targeting cancer cells by ROS-mediated mechanisms: a radical therapeutic approach? Nat Rev Drug Discov 2009; 8: 579-591.

[29] Du LY. Clinical observation on treating 52 cases of primary liver cancer diarrhea with Zuo zhu Daxi plus Fu zi Li zhong pill. Clinical Journal of Chinese Medicine 2011; 3: 35-36.

[30] Niu HX. Clinical observation on primary liver cancer with zhenwu decoction. Journal of Shanxi Traditional Chinese Medicine 2015; 36: 841-842.